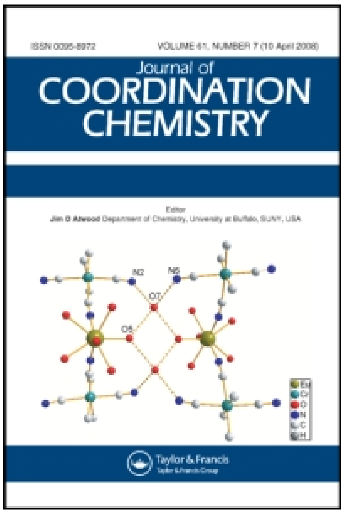

Journal of Coordination Chemistry
Publication details, including instructions for authors and subscription information:
http://www.informaworld.com/smpp/title~content=t713455674

STRUCTURAL, MAGNETOCHEMICAL, SPECTRAL AND THERMAL PROPERTIES OF *TRANS*-TETRAKIS(1,2-DIAZOLE) BISBROMOMANGANESE(II)

Paavo Lumme[a]; Eva Lindell[a]
[a] Division of Inorganic Chemistry, Department of Chemistry, University of Helsinki, Helsinki, Finland

To cite this Article Lumme, Paavo and Lindell, Eva(1987) 'STRUCTURAL, MAGNETOCHEMICAL, SPECTRAL AND THERMAL PROPERTIES OF *TRANS*-TETRAKIS(1,2-DIAZOLE) BISBROMOMANGANESE(II)', Journal of Coordination Chemistry, 15: 4, 383 — 392

To link to this Article: DOI: 10.1080/00958978708079795

URL: http://dx.doi.org/10.1080/00958978708079795

J. Coord. Chem. 1987, Vol. 15, p. 383-392
Photocopying permitted by license only

STRUCTURAL, MAGNETOCHEMICAL, SPECTRAL AND THERMAL PROPERTIES OF *TRANS*-TETRAKIS(1,2-DIAZOLE) BISBROMOMANGANESE(II)

PAAVO LUMME† and EVA LINDELL

Division of Inorganic Chemistry, Department of Chemistry, University of Helsinki, Vuorik. 20, SF-00100 Helsinki, Finland

(Received May 22, 1986)

The crystal structure of *trans*-tetrakis(1,2-diazole)bisbromomanganese(II) was solved by direct methods using single-crystal X-ray (Mo-Kα) diffractometer data and refined to R = 0.054 for 1270 unique reflections with $I > 2\sigma(I)$. The compound crystallized from water as almost colourless, monoclinic prisms in space group C2/c (No. 15) with unit cell dimensions $a = 14.208(2)$, $b = 9.454(1)$, $c = 15.015(3)$Å, $\beta = 118.68(1)°$, $Z = 4$. The structure is formed from $[(C_3H_4N_2)_4(Br)_2Mn]$ molecular units held together through stacking of the 1,2-diazole rings approximately in the *b*-direction and weak van der Waals forces and hydrogen bonds. The coordination sphere around the Mn^{2+} ion is weakly distorted octahedral with two pairs of *trans*-positioned 1,2-diazole molecules at distances Mn–N(1) = 2.246(7) and Mn–N(3) = 2.229(6) Å, respectively, in the basal plane and the Br^- ions occupying the apical positions at a distance Mn–Br(1) = 2.729(1)Å. The angles Br(1)–Mn–N(1), Br(1)–Mn–N(3) and N(1)–Mn–N(3) are 91.2(1), 89.6(1) and 87.8(2)°, respectively. The 1,2-diazole rings are practically planar, but slightly tilted (N(1) and N(3) containing rings are at angles of 89.9(3) and 86.4(3)° with respect to the basal coordination plane). The molecular units form columns in the *b*-direction. The molar magnetic susceptibilities, corrected for diamagnetism by Pascal's constants, at 93–303 K show the compound to be of high-spin complex type with a Curie-Weiss equation $\chi'_M = 4.30/(T-3.3)$ and the reflectance spectrum in accordance with this shows only a very weak shoulder at 23500 cm^{-1} corresponding to the $^6A_{1g} \rightarrow {}^4T_{2g}$ transition for the Mn^{2+} ion. The infrared spectrum shows an Mn–Br band at 715 and Mn–N bands at 680, 600 and 580 cm^{-1}. The thermogravimetric (TG) curve shows the complex to release the 1,2-diazole molecules in two steps in accordance with the structure.

Key words: manganese, 1,2-diazoles, structure, magnetochemistry, properties

INTRODUCTION

The importance of the manganese(II) ion in biological systems was recognized about fifteen years ago,[1] but extensive studies of relevant manganese(II) complexes have received limited attention until the ten years. Among the studied complexes those of imidazole and 1,2-diazole and their derivatives have been most investigated due to their possible effectiveness in physiological processes.[1]

To add to our basic knowledge on properties of the latter complexes we have recently prepared several manganese(II) complexes of 1,2-diazole, solved their crystal structures and verified their magnetic, spectral and thermal properties.[2,3] This has now been extended to a dibromo complex and the results are reported below and compared with earlier findings.

---

†Author for correspondence.

EXPERIMENTAL

Materials, Preparation of the Complex and Analyses.

$MnCl_2 \cdot 4H_2O$ (7.42 g, 0.0375 mol) in water (15 cm^3) was added with stirring to a hot aqueous solution (90 cm^3) of 1,2-diazole (10.2 g, 0.15 mol), KBr (44.64 g, 0.375 mol) and few drops of 2 M HCl. The complex crystallized on cooling and was allowed to stand in solution several days. The crystals were filtered on a sinter, washed with cold water (5°C) and dissolved in few cm^3 of dilute HCl. After some days almost colourless prismatic crystals separated, and these were filtered and stored in a desiccator. For analysis, manganese was determined by EDTA titration[4] and bromide by potentiometric titration with known NaOH solution after elution of the complex solution through a cation exchanger. Anal; Calcd. for $C_{12}H_{16}N_8Br_2Mn$: Mn, 11.3; Br, 32.8 %. Found: Mn, 11.15; Br, 32.8%.

Crystal Data

$C_{12}H_{16}N_8Br_2Mn$, M = 487.1. Monoclinic, a = 14.208(2), b = 9.454(1), c = 15.015(3) Å, β = 118.68(1)°, V = 1769.4(5) $Å^3$ (by least-squares refinement for 25 automatically centred reflections, $\lambda(\text{Mo-}K\alpha) = 0.71069$ Å), space group $C2/c$ (No. 15), $Z = 4$, $D_X = 1.80$, $D_c = 1.83$ Mgm^{-3}, $F_{000} = 956$, $\mu(\text{Mo-}K\alpha) = 5.58$ mm^{-1}.

Data Collection and Structure Determination

The crystal selected for intensity data collection had dimensions 0.3 × 0.3 × 0.4 mm and was sealed in a Lindemann glass capillary. The unit cell parameters were determined by least-squares treatment of the adjusted angular settings of 25 reflections measured on a NICOLET P3F diffractometer. The intensity measurements were carried out at room temperature (22± 1°C) with graphite-monochromated Mo-$K\alpha$ radiation and using the ω-2θ scan technique. The scan rate varied from 2.0 to 29.3° min^{-1}, depending on the number of counts measured in a fast preliminary scan through the peak. A set of 2030 unique reflections was obtained from the 2310 reflections measured from the minimum value (3°) up to the maximum value of $2\theta = 55°$. 1270 reflections with $I > 2\sigma(I)$ were considered as observed and used in the refinement. One strong reflection monitored periodically exhibited no significant variation of intensity. The intensities

TABLE I
Fractional atomic coordinates ($\times 10^4$) and equivalent values of the anisotropic temperature factor coefficients[a] ($\times 10^4$) of non-hydrogen atoms with e.s.d.'s in parentheses

Atom	*x/a*	*y/b*	*z/c*	U_{eq}($Å^2$)
Mn	2500(0)	2500(0)	5000(0)	301(9)
N(1)	2448(5)	2325(6)	6467(4)	345(36)
N(2)	3107(5)	2986(7)	7337(6)	538(46)
N(3)	3621(4)	663(7)	5508(4)	336(34)
N(4)	4690(5)	824(7)	6033(5)	536(42)
C(1)	2849(9)	2615(11)	8091(6)	674(69)
C(2)	2022(8)	1750(10)	7651(9)	648(73)
C(3)	1778(6)	1581(7)	6663(6)	330(45)
C(4)	5186(7)	−441(10)	6304(8)	685(64)
C(5)	4427(7)	−1434(9)	5966(7)	588(59)
C(6)	3467(6)	−699(9)	5473(6)	451(48)
Br(1)	4214(1)	4291(1)	5864(1)	511(5)

[a] $U_{eq} = (1/3)\Sigma_i\Sigma_j U_{ij} a_i^* a_j^* a_i \cdot a_j$.[11]

were corrected for Lorentz, polarization and absorption effects but corrections for extinction were considered unnecessary.

The space group $C2/c$ was assigned on the basis of the isomorphous structure of the chloro complex[5] and the complete structure analysis. Using the atom positions of the chloro complex[5] as the starting values the coordinates of the non-hydrogen atoms were verified by successive Fourier syntheses. With anisotropic temperature factors for the non-hydrogen atoms, a difference map calculated after full-matrix refinement revealed the positions of all eight hydrogen atoms. Full-matrix least-squares refinement with all non-hydrogen atoms given anisotropic temperature factors and hydrogen atoms at calculated positions (N–H and C–H = 1.000 Å) with uniform isotropic thermal parameters ($U = 0.05$ Å^2) led to $R = \Sigma((|F_o| - |F_c|)/|F_o|) = 0.054$ and $R_w = (\Sigma w(|F_o| - |F_c|)^2/\Sigma w|F_o|^2)^{1/2} = 0.048$, where $w = 1/\sigma(F_o^2)$. After the last cycle (with the hydrogen atoms fixed) the average shift/error was 0.001152 and maximum shift/error 0.005423. A final difference map was practically featureless.

Scattering factors were taken from Cromer and Mann[6] and the anomalous dispersion correction was applied.[7] All calculations were performed on a Univac 1100/61 EI computer using X-RAY 76 by Stewart[8]; for planes a program MPLN by Truter[9] was used.

The fractional atomic co-ordinates with the equivalent values of the anisotropic temperature factor coefficients for non-hydrogen atoms are given in Table I and for hydrogen atoms in Table II. The anisotropic thermal parameters and lists of the observed and calculated structure factors are available as supplementary material from the Editor-in-Chief upon request.

Physical Measurements

Magnetic susceptibilities were measured by the Gouy method at 93.2–303.2 K as described in reference 2. The calculated diamagnetic correction used was -241.8×10^{-6} e.m.u. The calibration standard was $HgCo(NCS)_4$.[10] The magnetic susceptibility data are mean values from measurements in three magnetic fields.

Infrared spectra were recorded in KBr disks (1.7 mg of the compound: 200.7 mg of KBr) on a Perkin-Elmer 577 Grating Infrared Spectrophotometer; diffuse reflectance spectra were measured on a Beckman DK-2A spectrophotometer as described in reference 2.

TG curves were run on a Mettler TA 3000 Thermal Analyses System equipped with a TG 50 Thermobalance and TC 10 TA Processor. The sample weighed 11.011 mg, the cups used were of alumina, the heating rate was 5°C min^{-1} and the atmosphere was

TABLE II

Fractional atomic coordinates (x10^4) calculated for hydrogen atoms keeping the non-hydrogen atoms fixed, U(H) = 0.05 Å^2 and N–H and C–H = 1.000 Å.

Atom	x/a	y/b	z/c
H(1)	3697	3647	7431
H(2)	3214	2937	8814
H(3)	1639	1295	7987
H(4)	1180	982	6157
H(5)	5069	1756	6200
H(6)	5978	−604	6689
H(7)	4528	−2482	6050
H(8)	2745	−1159	5130

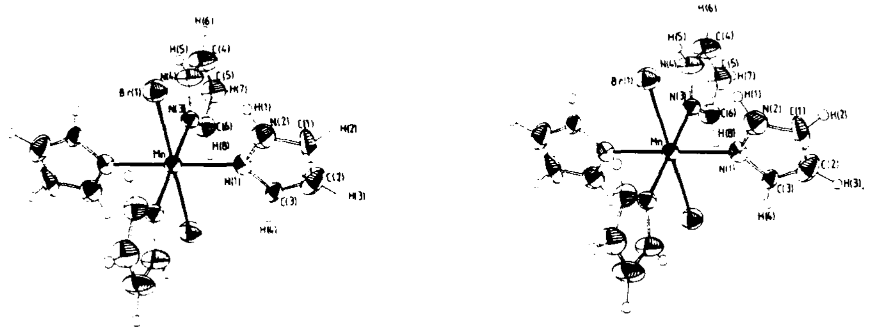

FIGURE 1 An ORTEP drawing of the $Mn(C_3H_4N_2)_4Br_2$ complex (with 295 K parameters) showing the molecular geometry and atom numbering scheme. Thermal ellipsoids are drawn at 50% probability level for the non-hydrogen atoms.

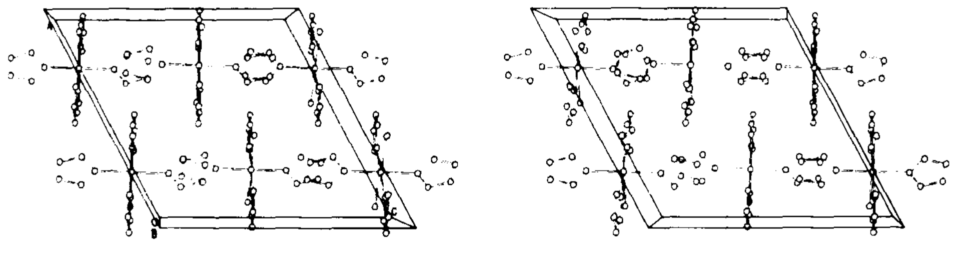

FIGURE 2 Stereo arrangement of the molecules in the unit cell of $Mn(C_3H_4N_2)_4Br_2$ viewed down *b*.

nitrogen (99.998 % N_2), with a flow rate of 70 cm^3 min^{-1}. The kinetics of the reactions were calculated in the conversion range $\alpha = 0.1-0.8$.

Densities of the crystals were determined by the flotation method in toluene - CH_2I_2.

RESULTS AND DISCUSSION

Description of the Structure and Comparisons

Stereo views of the ORTEP drawings[12] of the molecular unit and of the molecular packing in the unit cell are shown in Figures 1 and 2, respectively.

The coordination sphere around the manganese(II) ion is weakly distorted octahedral (Figure 1; Table III), the coordinating pyridine nitrogen atoms N(1), N(11), N(3) and N(13) situated in the basal plane and the bromide ions Br(1) and Br(11) taking the apical positions. The manganese(II) ion is placed in the basal plane (Table IV). Both of the 1,2-diazole rings are practically planar (Table IV) and are tilted with respect to each other with an angle of 83.8(4)°. The N(1)- and N(3)-containing 1,2-diazole rings are at angles 89.9(2) and 86.4(3)°, respectively, with respect to the basal plane. On the other hand the basal plane and the N(1)- and N(3)-containing 1,2-diazole rings are inclined at angles 51.3(1), 38.9(3) and 87.5(3)°, respectively, towards the *ac*-plane. The planes Br(1)N(1)MnN(11)Br(11) and Br(1)N(3)MnN(13)Br(11) are calculated to be at an angle of 87.8(1)° to each other and at angles 89.5(1) and 88.8(1)°, respectively, with respect to the basal plane (Table IV).

TABLE III

Bond distances (Å) and angles (°) with e.s.d.'s in parentheses.

Symmetry code			
Superscript			
None	X	Y	Z
i	0.5-X	0.5-Y	1-Z
Manganese coordination sphere			
Mn-N(1)	2.246(7)	Mn-N(1)-C(3)	128.4(5)
Mn-N(3)	2.229(6)	Mn-N(1)-N(2)	125.8(6)
Mn-Br(1)	2.729(1)	Mn-N(3)-N(4)	122.3(5)
		Mn-N(3)-C(6)	132.7(5)
(Uncoordinated)			
Mn-N(2)	3.219(9)	N(1)-Mn-N(3)	87.8(2)
Mn-N(4)	3.158(6)	N(1)-Mn-N(3)^{i}	92.2(2)
Mn-C(3)	3.24(1)	N(1)-Mn-Br(1)	91.2(1)
Mn-C(6)	3.253(9)	N(1)-Mn-Br(1)^{i}	88.8(1)
		N(3)-Mn-Br(1)	89.6(1)
		N(3)-Mn-Br(1)^{i}	90.4(1)
1,2-Diazole Ligands			
(Ring 1)			
N(1)-N(2)	1.341(8)	N(1)-N(2)-C(1)	110.0(7)
N(2)-C(1)	1.391(16)	N(2)-C(1)-C(2)	105.5(9)
C(1)-C(2)	1.320(14)	C(1)-C(2)-C(3)	109(1)
C(2)-C(3)	1.362(16)	C(2)-C(3)-N(1)	110.2(7)
C(3)-N(1)	1.325(11)	C(3)-N(1)-N(2)	105.8(7)
(Ring 2)			
N(3)-N(4)	1.343(8)	N(3)-N(4)-C(4)	110.9(6)
N(4)-C(4)	1.35(1)	N(4)-C(4)-C(5)	107.5(7)
C(4)-C(5)	1.33(1)	C(4)-C(5)-C(6)	105.0(7)
C(5)-C(6)	1.39(1)	C(5)-C(6)-N(3)	111.8(7)
C(6)-N(3)	1.30(1)	C(6)-N(3)-N(4)	104.8(6)
Hydrogen atoms			
(Ring 1)			
N(2)-H(1)	1.000(7)	N(1)-N(2)-H(1)	125.0(9)
C(1)-H(2)	1.000(8)	C(1)-N(2)-H(1)	125.0(7)
C(2)-H(3)	1.000(14)	N(2)-C(1)-H(2)	127(1)
C(3)-H(4)	1.000(6)	C(2)-C(1)-H(2)	127(1)
		C(1)-C(2)-H(3)	126(1)
		C(3)-C(2)-H(3)	125.7(8)
		C(2)-C(3)-H(4)	124.9(9)
		N(1)-C(3)-H(4)	124.9(9)
(Ring 2)			
N(4)-H(5)	1.000(7)	N(3)-N(4)-H(5)	124.5(6)
C(4)-H(6)	1.000(9)	C(4)-N(4)-H(5)	124.5(6)
C(5)-H(7)	1.000(9)	N(4)-C(4)-H(6)	126.3(8)
C(6)-H98)	1.000(8)	C(5)-C(4)-H(6)	126.3(9)
		C(4)-C(5)-H(7)	127.5(8)
		C(6)-C(5)-H(7)	127.5(8)
		C(5)-C(6)-H(8)	124.1(8)
		N(3)-C(6)-H(8)	124.1(7)

TABLE IV
Analyses of the most significant planes with displacements of each atom. The e.s.d.'s are given in parentheses.

Plane	N(1)N(3)N(11)N(13)Mn	$0.64896X + 0.62535Y + 0.43335Z = 4.29915$[a]
	N(1). N(3). N(11). N(13) all 0.000(6). Mn = 0.000(0)	
Plane	N(1)N(2)C(1)C(2)C(3)	$-0.57164X + 0.77854Y - 0.25906Z = 0.18649$
	N(1) −0.006(8). N(2) 0.006(7). C(1) −0.004(11). C(2) 0.000(10). C(3) 0.004(8)	
Plane	N(3)N(4)C(4)C(5)C(6)	$-0.51660X + 0.04443Y + 0.85508 Z = 5.62797$
	N(3) −0.003(7). N(4) 0.006(7). C(4) −0.006(10). C(5) 0.003(9). C(6) −0.000(8)	

[a] X. Y. Z are the fractional coordinates in direct space.

TABLE V
Distances and angles in interactions of the type D–H . . . A.

D	H	A	D–H (Å)	D . . . A (Å)	H . . . A (Å)	D–H . . . A (°)
N(2)	H(1)	Br(1)	1.000(7)	3.498(10)	2.847(1)	123.4
N(4)	H(5)	Br(1)	1.000(7)	3.334(7)	2.623(1)	127.9(4)
C(3)	H(4)	$Br(1)^{i}$	1.000(6)	3.453(8)	2.821(1)	121.7
C(6)	H(8)	$Br(1)^{i}$	1.000(7)	3.598(8)	3.017(1)	118.1
N(2)	H(1)	$Br(1)^{ii}$	1.000(7)	3.668(6)	2.906(1)	133.6

Symmetry position of atom A: (i) 0.5–X. 0.5–Y. 1–Z: (ii) 1–X. Y. 1.5–Z.

TABLE VI
Comparison of the unit cell and the M–X. M–N(1) and M–N(3) bond lengths (Å) in some 1.2-diazole complexes.[a,b]

Compound	*a*	*b*	*c*	β(°)	M–X	M–N(1)	M–N(3)
$Mn(HPz)_4Br_2$	14.208(2)	9.454(1)	15.015(3)	118.68(1)	2.729(1)	2.246(7)	2.229(6)
$Mn(HPz)_4Cl_2$[5]	13.695(3)	9.426(2)	15.239(2)	118.03(1)	2.579(1)	2.249(2)	2.229(2)
$Mn(HPz)_4(NCS)_2$[2]	11.485(4)	12.513(4)	14.554(11)	105.04(5)	2.202(6)	2.247(5)	2.237(5)
$Mn(MPz)_4Br_2$[13,c]	8.802(6)	9.695(5)	7.613(8)	114.98(4)	2.727(2)	2.256(3)	2.243(3)
$Ni(HPz)_4Br_2$[14]	14.127(7)	9.334(3)	14.702(2)	118.62(3)	2.682(1)	2.101(4)	2.080(5)
$Ni(HPz)_4Cl_2$[15]	13.876(1)	9.263(6)	14.451(3)	116.83(1)	2.507(1)	2.097(2)	2.087(3)
$Ni(HPz)_4(ONO)_2$[16]	14.230(4)	9.747(3)	14.387(4)	117.85(2)	2.09(1)[d]	2.097(4)	2.079(4)
$Cu(HPz)_4Cl_2$[17]	13.657(5)	9.200(5)	14.900(5)	118.04(1)	2.840(1)	2.024(1)	2.009(1)

[a] HPz = 1,2-Diazole. MPz = 5-Methyl-1,2-diazole. [b] Space group for all complexes is *C*2/*c* (*Z* = 4). except for $Mn(MPz)_4Br_2$ when it is *P*1 (*Z* = 1). [c] (α = 105.12(4). γ = 92.90(3)). [d] 2.14(1).

By considering the molecular packing in the unit cell (Figure 2) the crystal structure is seen to be formed by separate molecular units which form columns in the *b*-direction. The structure is held together by weak van der Waals forces and a weak net of inter- and intramolecular hydrogen bonds (Table V).

The structure is thermally rather labile, but the temperature factors (Table I) and the thermal ellipsoids (Figure 1) are, however, of the same order of magnitude as those of isostructural complexes (Table VI).[2,5,14–17] These 1,2-diazole complexes, except for the species $Mn(MPz)_4Br_2$, have the same space group *C*2/*c*. The unit cell dimensions of the $Mn(HPz)_4(NCS)_2$ complex only differ with respect to the basic series. On the other hand it is interesting to observe how the insertion of only one methyl group in the 1,2-diazole ligand is enough to change the space group from *C*2/*c* to *P*1 for the $Mn(MPz)_4Br_2$ complex (Table VI).

TABLE VII

Inclination of the 1,2-diazole rings toward the X atoms occupying the apical positions in the coordination sphere of the central metal atom for some 1,2-diazole complexes.[a]

Compound	Δ_1(°) (Ring 1)	Δ_2(°) (Ring 2)
Mn(HPz)$_4$Br$_2$	2.6	10.4
Mn(HPz)$_4$Cl$_2$[5]	1.9	11.5
Mn(HPz)$_4$(NCS)$_2$[2]	7.7	1.7
Mn(MPz)$_4$Br$_2$[13]	9.4	10.4
Ni(HPz)$_4$Br$_2$[14]	1.7	11.3
Ni(HPz)$_4$Cl$_2$[15]	7.0	13.0
Ni(HPz)$_4$(ONO)$_2$[16]	7.2	6.5
Cu(HPz)$_4$Cl$_2$[17]	3.0	10.0

[a] Δ_1 = (C(3)-N(1)-M) - (N(2)-N(1)-M), Δ_2 = (C(6)-N(3)-M) - (N(4)-N(3)-M).

The M-N(1) and M-N(3) bond lengths (Table VI) are seen to be of the same order of magnitude in the same complex and decrease for different complexes in the order Mn>Ni>Cu. The M-X bond length, however, seems to depend both on the nature of X and the metal ion. The shortest M-X bond lengths are found in the nitrito Ni(HPz)$_4$(ONO)$_2$ and isotiocyanato Mn(HPz)$_4$(NCS)$_2$ complexes, which are least distorted, and longest in the chloro complex Cu(HPz)$_4$Cl$_2$, which is the most distorted from regular geometry.

The tendency to form hydrogen bonds between the coordinated X atom or group and the 1,2-diazole rings may be thought to correlate with their inclination toward each other.[13] The calculated angle differences Δ_1 = (C(3)-N(1)-M) - (N(2)-N(1)-M) and Δ_2 = (C(6)-N(3)-M) - (N(4)-N(3)-M) are taken to be measures of the inclination in question (Table VII). The angle differences correlate with the tendency of the 1,2-diazole rings to form hydrogen bonds with the X group. According to the values hydrogen bond formation would be about equally strong for both rings in Ni(HPz)$_4$(ONO)$_2$ and Mn(MPz)$_4$Br$_2$ complexes in accordance with the length of the hydrogen bonds in the structures.[16,13] In the other complexes (Table VII) the ring 2 would be the stronger hydrogen bonded, except in the case of the isothiocyanato complex for which the order is reversed. This complex, however, has only intramolecular hydrogen bonds.[2] These conclusions are also in agreement with the length of the hydrogen bonds in the structures if the hydrogen bond is considered to be the stronger, the shorter it is.[2,5,14,15,17]

Magnetic, Spectral and Thermal Properties

The susceptibility values for the title complex follow the Curie-Weiss law $\chi'_M = C/(T-\theta) = 4.300/(T-3.30)$ in the temperature range used (Table VIII). In accordance with this the effective magnetic moment μ_{eff} is practically constant and of the same order of magnitude as the spin-only value of 5.92 B.M. indicating that the orbital contribution is insignificant. This is also in agreement with the instability of the complex.

The assignments of the infrared bands (Table IX) are based on results concerning similar complexes[2] and the spectrum of 1,2-diazole.[18] The spectrum shows obviously a ν(M-Br) vibration at 715 cm^{-1} and ν(M-N) vibrations at 680, 600 and 580 cm^{-1}. The reflectance spectrum of the complex shows only a very weak shoulder at 23500 cm^{-1} which is assigned to the $^6A_{1g} \rightarrow {}^4T_{2g}$ transition for the Mn^{2+} ion.

TABLE VIII
Magnetic data for $Mn(C_3H_4N_2)_4Br_2$.

T(K)	χ'_M(exp.) x10^5 (cgs emu)	χ'_M(calcd) x10^5 (cgs emu)	μ_{eff} (B.M.)
93.2	4687(60)	4786	5.91(4)
103.2	4315(72)	4307	5.97(5)
113.2	3916(23)	3915	5.96(2)
123.2	3699(61)	3588	6.04(5)
133.2	3374(92)	3312	6.00(8)
143.2	3117(74)	3075	5.98(7)
153.2	2884(37)	2870	5.95(4)
163.2	2720(11)	2690	5.96(1)
173.2	2507(18)	2532	5.90(2)
183.2	2369(10)	2391	5.89(1)
193.2	2247(9)	2265	5.90(1)
203.2	2154(8)	2152	5.92(1)
213.2	2049(4)	2049	5.91(1)
223.2	1965(16)	1956	5.93(2)
233.2	1875(5)	1871	5.92(1)
243.2	1776(19)	1793	5.88(3)
253.2	1708(14)	1721	5.88(2)
263.2	1643(13)	1655	5.88(2)
273.2	1588(32)	1593	5.89(6)
283.2	1462(35)	1537	5.76(7)
293.2	1442(25)	1484	5.82(5)
303.2	1398(23)	1434	5.83(5)

TABLE IX
Observed infrared bands (cm^{-1}) in the $Mn(C_3H_4N_2)_4Br_2$ complex and their assignments.[a]

Band	Assignment	Band	Assignment	Band	Assignment
3335vsb	ν(NH)	1453s	δ(ring)	908s	δ(ring)
3280vs	ν(NH)	1395vs	δ(ring)	893m	δ(CH)
3125m	ν(CH)	342vs	δ(ring)	870vw	δ(CH)
3105s	ν(CH)	1253m	δ(CH)	858m	δ(CH)
2970w	c and o	1150s	δ(NH)	782vs	δ(CH)
2920w	c and o	1120vs	δ(NH)	768vs	δ(CH)
2850w	c and o	1110vs	δ(NH)	715s	ν(M-Br)
1745w	ν(ring)	1055vs	δ(CH)	680s	ν(M-N)
1622m	ν(ring)	1037vs	δ(CH)	645vw	δ(ring)
1513s	δ(ring)	937vs	δ(ring)	600s	ν(M-N)
1462vs	δ(ring)	920vw	δ(ring)	580s	ν(M-N)

[a] b = broad, m = medium, s = strong, sh = shoulder, v = very, w = weak, ν = stretching, δ = bending, c = combination, o = overtones

The thermal and kinetic data (Figure 3; Table X) compared with the U_{eq} (Table I) or $U_{eq}^{1/2}$ values suggest that the first two 1,2-diazole molecules lost were those coordinated through the N(1) and N(11) nitrogen atoms and in the second and third step those coordinated through the N(3) and N(13) atoms. The view is in agreement with the hydrogen bonding pattern (Tables V and VII) and the anisotropic temperature factor values. These results confirm the general conclusions drawn earlier in this respect.[2,3,5] The "reaction order" values, differing a little from zero, point to the fact that the loss of ligands is not purely dissociative but also involves diffusion.[19] The apparent activation energy and frequency factor values point to the equality of the N(3)- and N(13)-containing 1,2-diazole molecules although they are lost in a stepwise fashion.

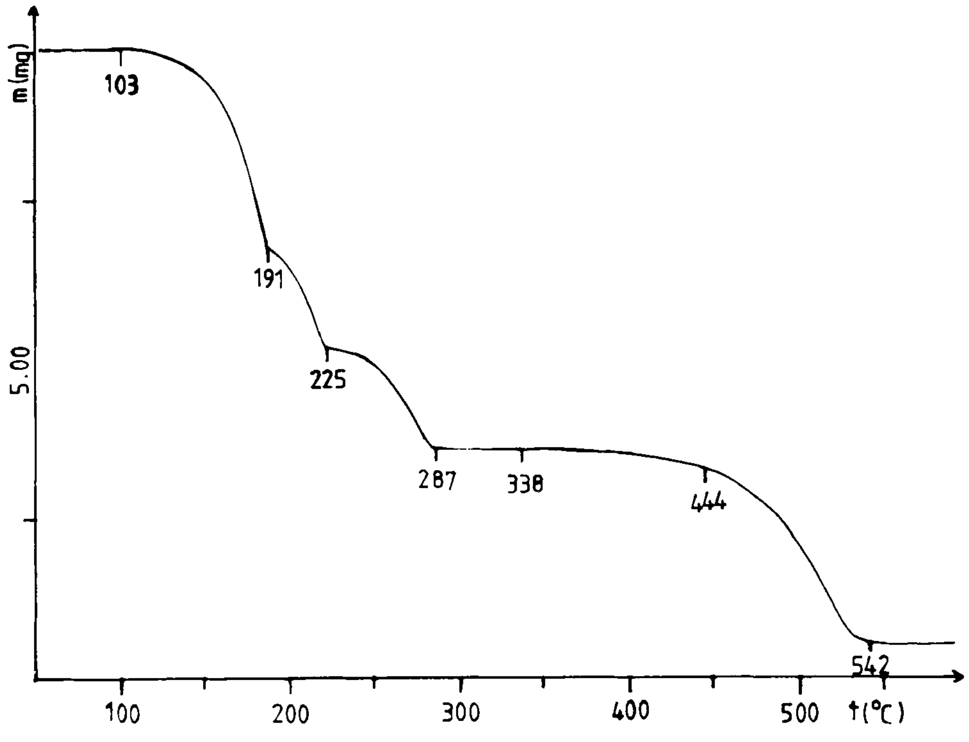

FIGURE 3 TG curve of $Mn(C_3H_4N_2)_4Br_2$ in a dynamic N_2 atmosphere.

The stability and decomposition temperature range of the $MnBr_2$ formed (Table X) differ considerably from results obtained earlier for $MnBr_2$ during decomposition of $MnBr_2 2H_2O$ in a dynamic nitrogen atmosphere.[20] This is obviously due to the nature and mass of the beginning compound and of the $MnBr_2$ formed. In the earlier study, the

TABLE X
TG data for $Mn(C_3H_4N_2)_4Br_2$.

Process	Temperature range (°C)	Residue (% from total) Found	Residue (% from total) Calculated	Reaction order n	Activation energy (kJ mol^{-1})	ln A_b^a
$Mn(C_3H_4N_2)_4Br_2$						
$\downarrow$-$2C_3H_4N_2$	103-191			0.15(2)	83(2)	16.4(5)
$Mn(C_3H_4N_2)_2Br_2$		71.5	72.0			
$\downarrow$-$C_3H_4N_2$	191-225			0.26(1)	121(2)	24.7(6)
$Mn(C_3H_4N_2)Br$		57.4	58.1			
$\downarrow$-$C_3H_4N_2$	225-287			0.22(1)	119(2)	20.5(4)
$MnBr_2$	287-444	43.2	44.1			
$\downarrow$-$Br_2 + N_2$	444-542			0.35(5)	144(7)	16(1)
MnN_2	542	18.0	17.0			

[a] A = the frequency factor ($k = A \times e^{-E_a/(RT)}$).

amount of $MnBr_22H_2O$ used was 309 mg, the N_2 flow was 40 cm^3 min^{-1} and the cup used was a porcelain crucible, whereas in the present study the complex weighed only 11 mg, the nitrogen flow was 70 cm^3 min^{-1} and the cup fabricated from alumina. In the earlier study[20] the $MnBr_2$ formed seemed to sublime to a considerable degree; this was not observed in the present case.

The final residue formed (Table X) is probably a mixture of manganese nitrides[21] rather than a pure compound such as MnN_2, in accordance with results in the literature.[21] The stable nitride with highest nitrogen content reported in the literature[21] is Mn_6N_5 for which the calculated residue would be only 13.7 in the present case (Figure 3). For $MnO_{1.5}$ and MnO_2 the residues are 16.2 and 17.9%, respectively, but their formation would not be likely given in the experimental conditions employed.

REFERENCES

1. Metal Ions in Biological Systems, Ed. H. Sigel. (Marcel Dekker, INC, New York - Basel). Vols. **3** (1974), **6** (1976), **8-10** (1979-80) and **12-15** (1981)-83; Harpers Review of Biochemistry, Eds. D.W. Martin, Jr., P.A. Mayes and V.W. Rodwell, 19th Ed., (Lange Medical Publ., Los Altos, California, 1983).
2. P. Lumme, I. Mutikainen and E. Lindell, *Inorg. Chim. Acta*, **71**, 217 (1983).
3. P.O. Lumme, *Thermochim. Acta*, **85**, 101 (1985).
4. A.I. Vogel, 'Quantitative Inorganic Analysis', 3rd Edition, (Longmans, London, 1961), p. 434.
5. P.O. Lumme, E. Lindell and P.-R. Kivimäki, *XI. Nordiske Strukturkjemikermöte*, 1984, Tromsö, Norway, Abstracts, p. 33.
6. D.T. Cromer and J.B. Mann, *Acta Cryst.*, **A24**, 321 (1968).
7. 'International Tables for X-ray Crystallography', Vol. IV, (Kynoch Press, Birmingham, 1974).
8. J.M. Stewart, 'The XRAY system - version of 1976', Tech. Rep. TR-446, Computer Science Center, Univ. of Maryland, College Park, Maryland, U.S.A.
9. M.R. Truter and B.L. Vickery, *J. Appl. Cryst.*, **6**, 323 (1973), Program No. 124.
10. J.-C.G. Bünzli, *Inorg. Chim. Acta*, **36**, L413 (1979).
11. W.C. Hamilton, *Acta Cryst.*, **12**, 609 (1959).
12. C.K. Johnson, ORTEP (1965), Report ORNL-3794, Oak Ridge National Laboratory, Tennessee, U.S.A.
13. J. Redijk, B.A. Stork-Blaisse and G.C. Verschoor, *Inorg. Chem.*, **10**, 2594 (1971).
14. A.D. Mighell, C.W. Reimann and A. Santoro, *Acta Cryst.*, **B25**, 595 (1969).
15. C.W. Reimann, A.D. Mighell and F.A. Mauer, *Acta Cryst.*, **23**, 135 (1967).
16. A.J. Finney, M.A. Hitchman, C.L. Raston, G.L. Rowbottom, B.W. Skelton and A.H. White, *Aust. J. Chem.*, **34**, 2095 (1981).
17. A. Mighell, A. Santoro, E. Prince and C. Reimann, *Acta Cryst.*, **B31**, 2479, (1975).
18. A. Zecchina, L. Cerruti, S. Coluccia and E. Borello, *J. Chem. Soc. B*, 1363 (1967).
19. C.H. Bamford and C.F.H. Tipper, 'Comprehensive Chemical Kinetics, Vol. 22, Reactions in the Solid State', (Elsevier Sci. Publ. Co., Amsterdam-Oxford-New York, 1980).
20. P. Lumme and M.-T. Raivio, *Suomen Kemistilehti*, **B41**, 194 (1968).
21. Gmelins Handbuch der anorganischen Chemie, Mangan, Teil C3, 8 Aufl., (Springer-Verlag, Berlin-Heidelberg-New York, 1975), p. 231.